ELSEVIER

Microporous and Mesoporous Materials 47 (2001) 127–134

MICROPOROUS AND MESOPOROUS MATERIALS

www.elsevier.com/locate/micromeso

Preparation of thin supported MFI membranes by in situ nucleation and secondary growth

C. Algieri [a], G. Golemme [b,*], S. Kallus [c,1], J.D.F. Ramsay [c]

[a] *Istituto di Ricerca su Membrane e Modellistica di Reattori Chimici, IRMERC-CNR, Via P. Bucci, I-87030 Rende, Italy*
[b] *Dipartimento di Ingegneria Chimica e dei Materiali, Università della Calabria, Via Pietro Bucci, I-87030 Rende, Italy*
[c] *Laboratorie des Matériaux et Procédés Membranaires – LMPM, UMR 5635, CNRS, 1919 Route de Mende, F-34293 Montpellier, France*

Received 13 February 2001; received in revised form 30 May 2001; accepted 18 June 2001

Abstract

Tubular MFI zeolite membranes have been prepared in two steps with a modification of the secondary growth method. The first synthetic step is only devoted to the in situ nucleation of the molecular sieve, directly on the surface of the tubular ceramic UF support, and the bulk of the membrane is then grown on it under different conditions. The right choice of the synthetic parameters (composition of the synthetic clear solutions, temperature) enables one to obtain membranes with high gas permeability and sustained selectivity. The preliminary gas transport results and the morphology are compared with the ones from a membrane obtained in one step: permeability increases by almost one order of magnitude. SEM observations indicate the presence of a very thin (1–2 μm) MFI zeolite layer on the tubular support. The method illustrated in this work is an easy way to skip the deposition of pre-formed nano-sized crystals on tubular supports before the secondary growth of the MFI membrane.

Keywords: Tubular zeolite membrane; MFI zeolite; In situ nucleation; Secondary growth; Pure gas permeation

1. Introduction

Zeolite membranes have high thermal, chemical and structural stability, and for this reason they can be used at high temperatures and with organic solvents, when polymeric membranes cannot operate. The crystalline nature of zeolites offers a unique opportunity to obtain membranes with monodimensional pore sizes, which are therefore capable of separating mixtures of substances on the basis of differences in the molecular size and shape with extremely high selectivity. This is the case of zeolite A membranes, which became recently commercially available for high-temperature pervaporation: Mitsui Engineering and Shipbuilding Co. first installed a commercial plant made up of 16 zeolite A tubular membrane modules which produces 600 l/h of dehydrated solvents (ethanol, 2-propanol, acetone, etc.) containing less than 0.2% of water from feeds at 120°C containing

* Corresponding author. Tel.: +39-0984492010; fax: +39-0984492058.
E-mail address: ggolemme@unical.it (G. Golemme).
[1] Present address: Refining Catalyst Europe – GRACE Davison, In der Hollerhecke 1, D-67545 Worms, Germany.

1387-1811/01/$ - see front matter
PII: S1387-1811(01)00393-6

10% of water [1]. The high selectivity makes zeolite membranes also good candidates for the construction of membrane reactors. New promising applications include the reverse osmosis of organic solutions [2] which would spoil organic membranes.

Self-standing zeolite layers larger than a few square centimeters are difficult to form, and the resulting structures are fragile [3]. Therefore, zeolite membranes are typically deposited on mechanically resistant porous supports (alumina, stainless steel, etc.) [4]. The technical problem in the development of supported zeolitic membranes lies in the large thickness (typically 50 μm) required to obtain defect-free samples, that is the presence of defects in very thin layers.

The preparation strategies for zeolite membranes and the transport behavior of penetrants through them has been reviewed in an excellent paper by Caro et al. [5]. The usual one-step method to prepare zeolitic membranes consists in immersing the support in a suitable hydrothermal system, and repeating the deposition if the membrane is defective [6]. In some cases the solvent, and also the templating species, for the hydrothermal transformation of the precursor substances into the zeolitic membrane come from the vapor phase: Matsukata et al. [7], for instance, coated a porous alumina plate with an aluminosilicate gel and treated it with vapors of water and of templating amines, obtaining zeolitic membranes about 40 μm thick. The one-step method tends to produce rather thick layers, but the quality of the membrane, indicated by the ability to reject molecules larger than the pore size of the zeolite crystals and by the ability to undergo repeated heating cooling cycles, can be very high, due also to the fact that a significant part of the membrane can fill the pore system of the support [4].

The secondary growth method consists in the separation of the nucleation step from the crystal growth, and looks promising in the preparation of thin and defect-free zeolite membranes because it enables to optimize the conditions of each step independently. After the seeding of the support with crystallization nuclei or crystals, the growth of the membrane is carried out in a suitable hydrothermal system. It has been pointed out that the secondary growth method tends to produce thinner but less resistant and less selective zeolite membranes [4]. The nucleation step can be obtained in different ways. In one of them Balkus and co-workers deposited evaporated fragments of UTD-1 on a support kept at low temperature by pulsed laser ablation. A hydrothermal treatment on the support gave a homogeneous, compact and continuous UTD-1 membrane about 11 μm thick [8]. In another – more usual – approach to the nucleation step, nano-sized crystals of the desired zeolite are prepared apart and fixed to the support. Provided that a uniform and thin coverage of the support is obtained with the nano-crystals, this method potentially allows a better control of the thickness of the zeolite layer.

The reproducible deposition of a thin, compact and uniform nano-crystal layer on the surface of a tubular porous support, however, is by no means a trivial task. The most successful and reproducible deposition of colloidal nano-sized crystals is carried out on flat supports by spin coating, sedimentation/drying [9] or by careful soaking [10]: none of these methods is suitable for tubular membranes. In this work a new approach to nucleation is tested to overcome this difficulty. It consists of immersing a tubular ceramic support into a clear solution that favors the nucleation of silicalite-1 (MFI), with the aim to cover its surface with very small MFI crystals already bound to the ceramic matrix. The support is then washed and transferred to a different hydrothermal system, with lower supersaturation, for the secondary growth of the zeolite membrane. This method skips the task of pre-formed nano-sized crystals deposition. A potential advantage of the proposed approach is the possibility to have crystallization nuclei firmly attached to the ceramic matrix of the support, possibly deep into the pore system, and therefore with an intimate contact of the zeolite phase with the membrane support. In other words, the alternative secondary growth approach presented in this work might yield thin membranes with improved selectivity and resistance. MFI zeolite membranes with good fluxes and selectivities have been obtained via this approach. The flux improved with respect to a membrane obtained

with a literature one-step method, with no loss in selectivity.

2. Experimental

2.1. Materials

The supports used in this work are single-channel tubular membranes (od/id 10/7 mm) with 50 nm (α-Al_2O_3, SCT, France) and 60 nm (α-Al_2O_3, Inocermic GmbH, Germany) average pore size; the length of the tubes was in the range 5–10 cm, and their external surface was wrapped with Teflon tape before the introduction into the autoclaves. The chemicals were SiO_2 (Aerosil 380, Degussa, 95.5%), tetrapropylammonium hydroxide (TPAOH, 20 wt.% in water, Merck), tetraethoxysilane (TEOS, 98%, Janssen), sodium hydroxide (NaOH pellets, 97%, Carlo Erba) and distilled water. They were used as received with no further purifications. The gases used in the permeability tests were at least 99.99% pure.

2.2. Preparation of the MFI membrane with the one-step method (50(1))

The membrane was prepared according to the example described by Ramsay et al. [11]. A clear and homogeneous solution with the following molar ratio

$$25SiO_2 : 11.75TPAOH : 552H_2O$$

was obtained by adding a 20% TPAOH solution in water to the right amount of SiO_2 and stirring vigorously for 11 days at room temperature in a closed polyethylene bottle. The solution was poured into a Morey type Teflon-lined autoclave containing a 50 nm pore size support, and the hydrothermal synthesis was performed under autogenous pressure at 443 K for four days. After this time the composite membrane was washed repeatedly with distilled water up to neutral pH and dried at 379 K. The permeability of pure gases was tested in order to check the presence of defects. Then, the template TPA ion was calcined in static air according to the heating profile (I) reported in Fig. 1.

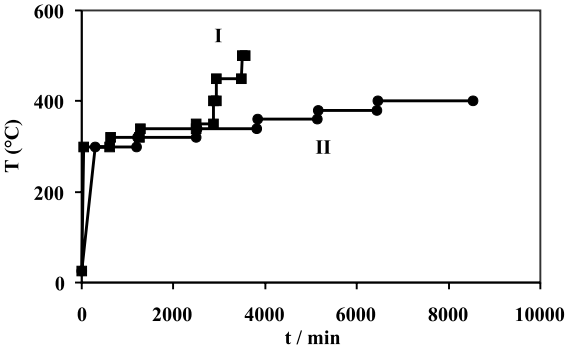

Fig. 1. Heating profiles for the calcination of the membranes; profile I: 50(1) (static air) and 50(2 + 1) (N_2 first, then repeated with static air) samples; profile II: 60(2 + 1) sample in static air.

2.3. Preparation of the first MFI membrane with the two-steps method (50(2 + 1))

A 50 nm pore size support was treated two times with a hydrothermal solution which favors the nucleation (solution I) and then with another solution which favors the growth of the crystals already present on the support (solution II).

The clear and homogeneous solution I with the following molar ratio [12]

$$25SiO_2 : 8.72TPAOH : 0.34NaOH : 449H_2O : 100EtOH$$

was obtained by adding TEOS, sodium hydroxide and distilled water to an aqueous 20% TPAOH solution contained in a closed polyethylene bottle, and stirring vigorously for 24 h at room temperature. The solution was poured into a Morey type Teflon-lined autoclave containing a 50 nm pore size support, and the hydrothermal treatment was performed at 363 K for 88 h. Then the composite membrane was washed repeatedly with distilled water up to neutral pH and dried at 313 K.

The nucleation procedure was repeated a second time with the same solution at the same temperature for 113 h. After washing and drying the sample was placed in an autoclave in contact with a more diluted, less alkaline, clear and homogeneous MFI precursor solution (solution II) with the following molar ratio [13]

$$25SiO_2 : 3.04TPAOH : 1454H_2O : 100EtOH$$

obtained by adding TEOS and aqueous TPAOH (20 wt.%) to distilled water in a closed polyethylene bottle, and stirring vigorously for 24 h at room temperature. The hydrothermal treatment was performed under autogenous pressure at 379 K for 66 h. Then the composite membrane was washed repeatedly with distilled water up to neutral pH and dried at 363 K. The permeability of pure gases was tested in order to check the presence of defects. The calcination of the template TPA ion was performed following the heating profile (I) reported in Fig. 1, at first in N_2 and then in static air.

2.4. Preparation of the second MFI membrane with the two-steps method (60(2 + 1))

A 60 nm pore size support was treated almost in the same way as the 50 nm support in the preparation of the 50(2 + 1) membrane. Solution I which was obtained in the same way, had the following molar ratio:

$$25SiO_2 : 8.82TPAOH : 0.31NaOH : 459H_2O : 100EtOH$$

and the hydrothermal treatment was performed at 363 K for 68 h. Then the support was washed repeatedly up to neutral pH and dried at 379 K. The nucleation procedure was repeated with the same solution at 376 K for 113 h, then the support was washed repeatedly up to neutral pH and dried at 385 K.

Finally, the sample was placed in an autoclave in contact with solution II, prepared in the same way as in the preparation of the 50(2 + 1) membrane, with the following molar ratio:

$$25SiO_2 : 3.02TPAOH : 1479H_2O : 100EtOH.$$

The hydrothermal treatment was performed at 413 K for 68 h. After repeated washings up to neutral pH and drying at 379 K, the permeability of pure gases was tested in order to check the presence of defects. Then, the template TPA ion was calcined up to 673 K in static air (heating profile II in Fig. 1).

2.5. Characterization of the supported MFI zeolite membranes

The pure gas permeance (P/l), before and after the calcination, was measured at room temperature with a volumetric method [14] through bubble flowmeters. The permeance at the steady state was calculated by the following equation:

$$P/l = n(\text{gas})/(\Delta p \Delta t A_m)$$

where Δp is the pressure gradient and A_m the area of the membrane. The ideal selectivity ($\alpha_{ij} = P_i/P_j$) was worked out as the ratio of the permeances at the steady state. The membranes were observed by using a Cambridge–Zeiss LEO 400 and a Cambridge Stereoscan 360 scanning electron microscope (SEM). Powder X-ray diffraction was performed on the material scratched off of the surface of the 50(1) sample with a Philips PW 1730/10 X-ray diffractometer using Ni-filtered Cu $K_{\alpha 1} + K_{\alpha 2}$ radiation ($\lambda = 1.542$ Å).

3. Results

3.1. Morphology and nature of the membranes

In Fig. 2 the top view of the 50 nm α-Al_2O_3 support (SCT) after the preparation and calcination of the 50(1) membrane is shown. Some loose objects (250–400 nm long, 80–130 nm wide) on the surface are visible, the coffin-like shape of which is

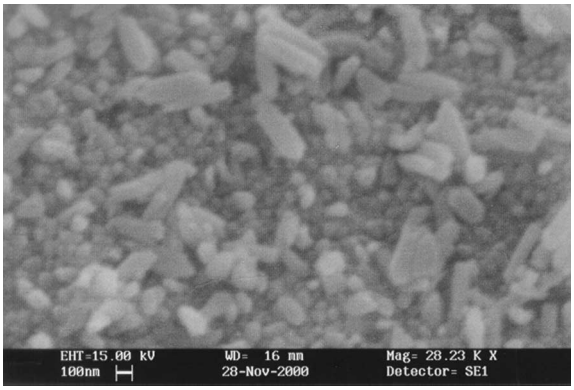

Fig. 2. Top view of the 50 nm α-Al_2O_3 support (SCT) after the preparation of the MFI 50(1) membrane.

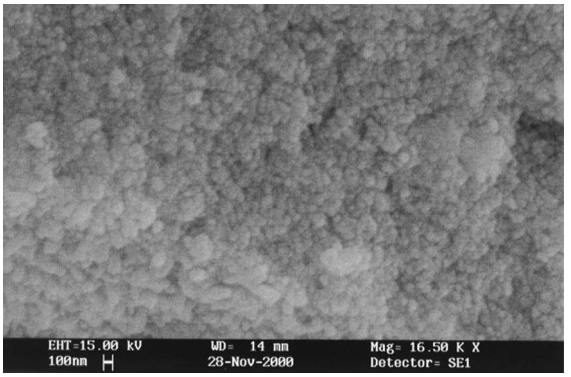

Fig. 3. Cross-section of the α-Al_2O_3 support (SCT) after the preparation of the MFI 50(1) membrane.

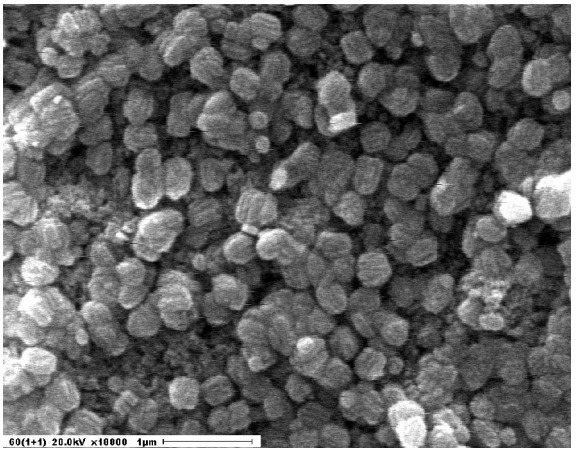

Fig. 5. Top view of the 60 nm α-Al_2O_3 support after the second nucleation step.

typical for MFI crystals. The cross-section (Fig. 3) shows that the open upper pores of the support have been filled in the 50(1) membrane. An evaluation of the thickness of the layer of the support which is completely filled is not easy, however it might be about 1–2 μm thick. After the permeance measurements the surface of the membrane was scratched off with a steel spatula, and its XRD powder pattern was measured. It was basically the diffractogram of α-Al_2O_3, but a weak signal at about $2\Theta = 23°$ corresponds to the most intense reflections of the MFI topology [16].

In Fig. 4 the top view (a) and the cross-section (b) of the calcined $50(2 + 1)$ membrane are shown. The membrane is a thin layer, about 0.8–1.0 μm thick, above the surface of the support, and it is built-up by the intergrowth of different crystalline domains with random orientation. In the lower left part of Fig. 4a a crack of the membrane is evidenced.

The evolution of the 60 nm α-Al_2O_3 support during the nucleation and crystal growth steps for the preparation of the $60(2 + 1)$ membrane was followed. Some MFI crystals, not larger than 200 nm, can be seen on the surface of the support after the first treatment at 363 K. After the second treatment for seeding at 379 K, the surface is almost evenly covered with a single layer of randomly oriented MFI crystals, the size of which is not larger than 400 nm (Fig. 5). The final treatment at 413 K with the clear solution of lower supersaturation yielded a thin layer, about 2.0 μm

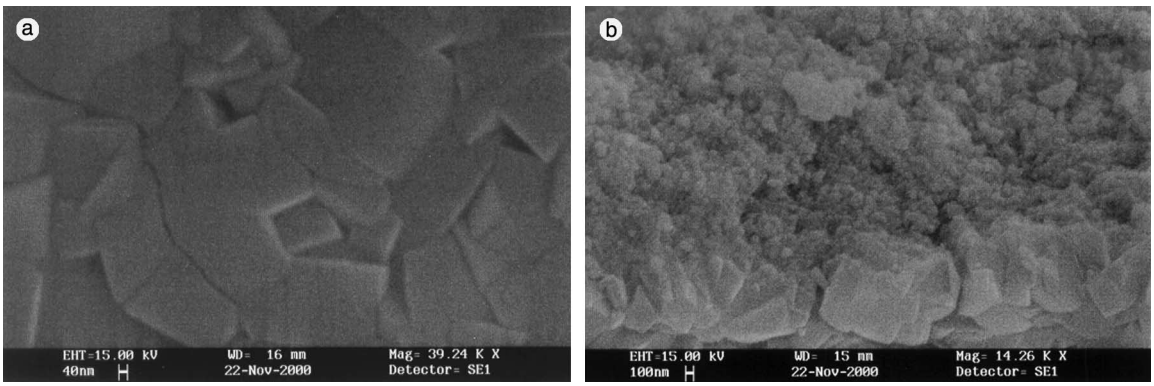

Fig. 4. (a) Top view and (b) cross-section of the $50(2 + 1)$ membrane.

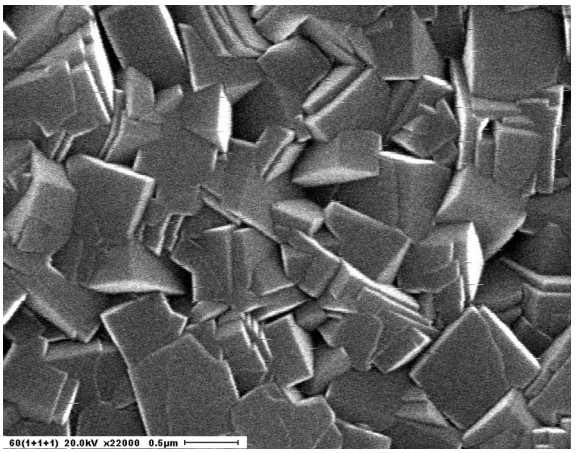

Fig. 6. Top view of the final 60(2 + 1) membrane prior to calcination.

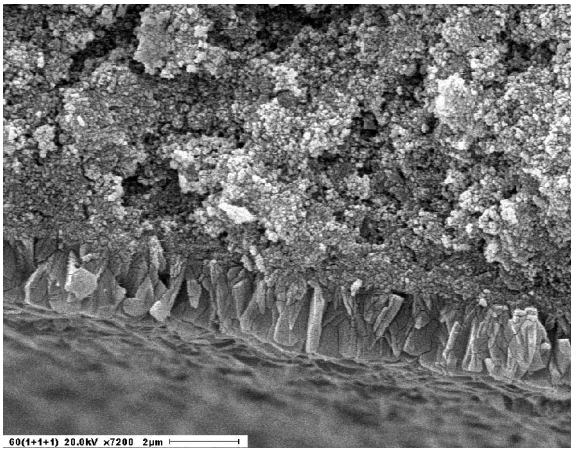

Fig. 7. Cross-section of the final 60(2 + 1) membrane prior to calcination.

thick, above the surface of the support, built-up by the intergrowth of different crystalline domains with random orientation (Figs. 6 and 7).

3.2. Single gas transport through the membranes

The pure gas permeance (He and N_2) was measured before the calcination of the membranes. N_2 permeance was below the detection limit for the 50(1) sample, and just detectable for He ($2–5 \times 10^{-13}$ mol/Pa s m^2 at 302.5 K, $\Delta p = 490$ kPa), indicating a perfect coverage. The N_2 permeance of

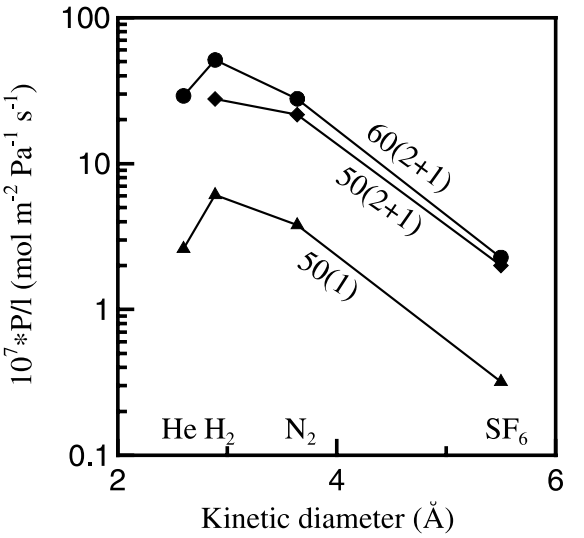

Fig. 8. Permeances of the MFI membrane: 50(1) ($\Delta p = 130$ kPa), 50(2 + 1) ($\Delta p = 98$ kPa), 60(2 + 1) ($\Delta p = 200$ kPa).

the 50(2 + 1) membrane was 1.08×10^{-9} mol/Pa s m^2 at 299 K and $\Delta p = 190$ kPa, indicating the presence of defects. The N_2 and He permeance of the 60(2 + 1) membrane was 1.55×10^{-12} and 1.35×10^{-11} mol/Pa s m^2, respectively, at 299 K and $\Delta p = 190$ kPa, indicating the presence of a negligible amount of defects.

The pure gas permeance of the three MFI membranes as a function of the kinetic diameter of the permeating species is shown in Fig. 8. Table 1 shows the ideal selectivities (ratios of pure gas permeances) of the membranes compared with the Knudsen selectivity.

4. Discussion

The morphology of the 50(1) MFI membrane (Fig. 3) is of the same kind as those obtained by Ramsay et al. [11] and by Julbe et al. [15] with the same synthesis solution but with a support of larger pore size and at a higher synthesis temperature (463 K). The MFI zeolite is in the pore system of the support, giving rise to a structure which is impermeable to He before the calcination of the organic template TPA ion occluded in the micropores. The pure gas transport properties after

Table 1
Pure gas transport properties at room temperature through the MFI membranes

Membrane	Δp (kPa)	P/l (H_2) (mol/s Pa m^2)	Ideal selectivity		
			H_2/He	H_2/N_2	H_2/SF_6
			1.41[a]	3.74[a]	8.54[a]
50(1)	130	6.09×10^{-7}	2.33	1.61	19.0
50(2 + 1)	98	27.7×10^{-7}	–	1.28	13.9
	130	35.4×10^{-7}	–	1.52	–
60(2 + 1)	200	48.5×10^{-7}	1.70	1.73	23.7

[a] Knudsen diffusion limit.

calcination (Fig. 8 and Table 1) are comparable to the values obtained by other authors with MFI membranes [9].

The 50(2 + 1) MFI membrane is more permeable but less selective than the 50(1) membrane, due to the presence of cracks in the zeolite layer (Fig. 4a). The H_2/SF_6 selectivity value, however, is still higher than the Knudsen diffusion limit.

The third membrane was prepared bearing in mind the limits of the 50(2 + 1) membrane: formation of cracks and, as a consequence, poor ideal gas selectivity. It has been evidenced that in the one-step synthesis higher temperatures improve the performance of the resulting MFI membranes [11]. In addition to this, Geus and van Bekkum suggested to limit the calcination temperature to 400°C in order to avoid the cracking of large MFI single crystals [17]. Therefore, an Inocermic support, made of the same material (α-Al_2O_3) and with a larger pore size (60 vs. 50 nm) than the SCT one, was used; the compositions of the synthesis solutions were the same as in the preparation of the 50(2 + 1) membrane; the main differences in the preparation of the 60(2 + 1) membrane with respect to the 50(2 + 1) sample was the higher temperature of the crystal growth step (413 vs. 379 K) and the new heating profile for the calcination, characterized by a lower maximum temperature (673 vs. 773 K, Fig. 1). Fig. 5 indicates that two nucleation treatments are required to effectively cover the surface of the 60 nm support with a layer of tiny MFI crystals, not larger than 400 nm. The pure gas permeability through the 60(2 + 1) MFI membrane is higher than in the case of both the 50(1) and the 50(2 + 1) membranes. In Fig. 8, where the permeance of the gases is reported versus the kinetic diameter for the three membranes, a very good similarity is found in the shape of the curves, especially for the two membranes of higher quality (50(1) and 60(2 + 1)). With reasonable confidence the transport mechanism is the same in both cases, but the membrane obtained by the secondary growth method (60(2 + 1)) is almost one order of magnitude more permeable. This fact may be in contradiction with the thickness of the two membranes, which is practically the same (1–2 vs. 2 μm). The nature of the two membranes, however, might explain the difference in permeability: the obstacle of the impermeable α-Al_2O_3 phase of the support, around the pores filled by the molecular sieve, reduces the active surface of the zeolite membrane, and increases its tortuosity, with an overall effect of slowing down the permeation through the 50(1) membrane.

The kinetic diameter of the SF_6 molecule (5.5 Å) is very close to the dimensions of the straight channels in the MFI crystals (5.4×5.6 Å^2) and larger than the sinusoidal channels (5.1×5.5 Å^2), therefore a certain sieving effect has to be expected. The ideal selectivity of all other gases with respect to SF_6, in fact, is always higher than the Knudsen diffusion limit, and is similar to the values found by other authors. Bai et al., [18] however, reported a higher H_2/SF_6 ideal selectivity (136) at room temperature with comparable H_2 permeance (34×10^{-7} mol/s Pa m^2) for a composite MFI/γ-Al_2O_3 membrane. Caro et al. [5], instead, report H_2/SF_6 and H_2/N_2 ideal selectivities of about 800 and 200, respectively, with a much lower H_2 permeance ($\sim 7.7 \times 10^{-9}$ mol/s Pa m^2) at 105°C, for a ZSM-5 membrane of columnar microstructure prepared by a seeding supported crystallization. The rather high SF_6 permeance of the membranes prepared in this study may be the indication of a certain

contribution of inter-crystalline space or pinholes to transport. As for as the H_2/He and H_2/N_2 ideal selectivities are concerned, a similar behavior is typical for MFI membranes prepared by a direct in situ crystallization [5,9]. A detailed picture of the gas transport properties of the membranes prepared in this study will be possible after permeation experiments at higher temperatures and with gas mixtures to be carried in our laboratory.

5. Conclusions

A method for the preparation of tubular MFI supported membranes is presented in which the in situ nucleation of MFI crystals on α-Al_2O_3 porous supports is followed by the secondary hydrothermal growth of the bulk of the membranes. Tubular MFI zeolite membranes with thicknesses in the range of 1–2 μm and high single gas (He, H_2, N_2, SF_6) flux and selectivity have been prepared. An effective control can be exerted independently on both the nucleation and the crystal growth. Preliminary pure gas permeation measurements at room temperature indicate that the selectivity of the membranes is improved by the control of the synthetic parameters (larger pore size of the support, higher temperature of the secondary growth, careful calcination). One of the MFI membranes obtained by secondary growth is as selective as a membrane obtained with a one-pot preparation in which the zeolite fills the pore network of the support, but its permeance is almost one order of magnitude higher.

Acknowledgements

Financial support of this work was provided by the Italian Ministry of University and S&T Research (in part through the former MURST 40% funds, and in part through the project P4WP1A2 "Sviluppo di materiali innovativi per ottica, elettro-ottica ed applicazioni civili e industriali – Membrane avanzate per la separazione di gas e liquidi). C.A. and G.G. are grateful to CNR and CNRS for two fellowships (CNR-CNRS 1998-99 scientific agreement). We thank Dr. D. Amori (Eigenmann & Veronelli SpA) for the gift of Aerosil 380, and Dr. M. Davoli, Dipartimento di Scienze della Terra – Università della Calabria, for the electron microscopy measurements.

References

[1] Y. Morigami, M. Kondo, J. Abe, H. Kita, K. Okamoto, Book of Abstracts of the 6th International Conference on Inorganic Membranes (ICIM6-2000), Montpellier (F), 26–30 June, 2000, p. 55.
[2] I. Kumakiri, T. Yamaguchi, S.I. Nakao, J. Chem. Eng. Jpn. 33 (2000) 333.
[3] T. Sano, Y. Kiyozumi, M. Kawamura, F. Mizukami, H. Takaya, T. Mouri, W. Inaoka, Y. Toida, M. Watanabe, K. Toyoda, Zeolites 11 (1991) 842.
[4] J. Coronas, J. Santamaria, Sep. Purif. Meth. 28 (1999) 127.
[5] J. Caro, M. Noack, P. Kölsch, R. Schäfer, Micropor. Mesopor. Mater. 38 (2000) 3.
[6] Z.A.E.P. Vroon, K. Keizer, A.J. Burggraaf, H. Verweij, J. Membr. Sci. 144 (1998) 65.
[7] M. Matsukata, N. Nishiyama, K. Ueyama, in: J. Weitkamp, H.G. Karge, H. Pfeifer, W. Hölderich (Eds.), Zeolites and Related Microporous Materials: State of the Art 1994, Studies in Surface Science and Catalysis, vol. 84, Part B, Elsevier, Amsterdam, 1994, p. 1183.
[8] K.J. Balkus Jr., T. Munoz Jr., M.E. Gimon-Kinsel, Chem. Mater. 10 (1998) 464.
[9] C.S. Tsay, A.S.T. Chiang, AICHE J 46 (2000) 616.
[10] G. Xomeritakis, S. Nair, M. Tsapatsis, Micropor. Mesopor. Mater. 38 (2000) 61.
[11] J.D.F. Ramsay, A. Giroir-Fendler, A. Julbe, J.A. Dalmon, FR Patent 9 405 562, 1994.
[12] A.E. Persson, B.J. Schoeman, J. Sterte, J.E. Otterstedt, Zeolites 14 (1994) 557.
[13] J. Hedlund, B.J. Schoeman, J. Sterte, in: H. Chou, S.-K. Ihm, Y.S. Uh (Eds.), Progress in Zeolite and Microporous Materials, Studies in Surface Science and Catalysis, vol. 105, Part A, Elsevier, Amsterdam, 1997, p. 2203.
[14] E. Drioli, S.-M. Zhang, A. Basile, G. Golemme, S.N. Gaeta, H.-C. Zhang, Gas Sep. Purif. 5 (1991) 252.
[15] A. Julbe, D. Farrusseng, J.C. Jalibert, C. Mirodatos, C. Guizard, Catal. Today 56 (2000) 199.
[16] E.M. Flanigen, J.M. Bennett, R.W. Grose, J.P. Cohen, R.L. Patton, R.M. Kirchner, J.V. Smith, Nature 271 (1978) 512.
[17] E.R. Geus, H. van Bekkum, Zeolites 15 (1995) 333.
[18] C. Bai, M.D. Jia, J.L. Falconer, R.D. Noble, J. Membr. Sci. 105 (1995) 79.